Materials Letters 223 (2018) 25–28

Contents lists available at ScienceDirect

Materials Letters

journal homepage: www.elsevier.com/locate/mlblue

Featured Letter

A high-permittivity and low-loss $(Ba_{1-x}Nd_x)(Ti_{1-y-x/4}Ce_y)O_3$ ceramic

Da-Yong Lu *, Yong-Shun Zheng

Research Center for Materials Science and Engineering, Jilin Institute of Chemical Technology, Jilin 132022, PR China

ARTICLE INFO

Article history:
Received 30 November 2017
Received in revised form 24 March 2018
Accepted 2 April 2018
Available online 3 April 2018

Keywords:
Barium neodymium titanate cerate
Ceramics
Defects
Dielectrics
Electron spin resonance

ABSTRACT

$(Ba_{1-x}Nd_x)(Ti_{1-y-x/4}Ce_y)O_3$ (BNTC) ceramics with a pseudo-cubic structure were prepared using the mixed oxide method. The dielectric-peak temperature decreased rapidly at a rate of −27 °C/at.% Nd for BNTC with $y = 0.05$. BNTC with $x = y = 0.05$ (BN5TC5) exhibited a high-permittivity diffuse phase transition behavior but had a higher dielectric loss ($\tan\delta = 0.219$). A high-permittivity ($\varepsilon'_{RT} = 14100$) and low-loss ($\tan\delta = 0.014$) X7V ceramic was achieved by means of the addition of 1% Ce in BN5TC5. A $g = 2.509$ electron spin resonance (ESR) signal associated with Ce^{3+} Kramers ions confirmed the existence of mixed valence states of Ce^{3+}/Ce^{4+}. A $g = 2.151$ ESR signal of Nd^{3+} can be detected at room temperature after these ceramics were preserved over a long period of time.

1. Introduction

Neodymium (Nd) and cerium (Ce) are two most abundant elements on earth among lanthanide [1]. Their application as dopants in $BaTiO_3$ dielectric ceramics has bright prospects. A similar material is high-permittivity $(Ba_{1-x}La_x)(Ti_{1-y-x/4}Ce_y)O_3$ ($x = 0.03$, $y = 0.05$) ceramic (BL3TC5) [2,3], in which La^{3+} were substituted exclusively for A-site [4–6] and Ce exhibited slight mixed valence states of Ce^{3+}/Ce^{4+} [7]. Cerium in $BaTiO_3$ is well known to exist as A-site Ce^{3+} [8], B-site Ce^{4+} [9], and mixed-valent Ce^{3+}/Ce^{4+} [10]. Nd^{3+} was generally considered to be substituted for A-site [11–13], whereas a self-compensation model in $(Ba_{1-x}Nd_x)(Ti_{1-x}Nd_x)O_3$ [14] and a slight amphoteric behavior of Nd^{3+} in $(Ba_{1-x}Nd_x)(Ti_{1-x}Ho_x)O_3$ [15] were discovered. In general, the asymmetric site occupations are apt to occur in Nd- or Ce-doped $BaTiO_3$, i.e., that Nd^{3+} favors A-site over B-site, whereas Ce favors B-site as Ce^{4+} over A-site as Ce^{3+}.

In this work, $(Ba_{1-x}Nd_x)(Ti_{1-y-x/4}Ce_y)O_3$ ceramics were reported. The general perspectives are to provide a novel high-permittivity and low-loss X7V ($-82\% \le (\varepsilon' - \varepsilon'_{RT})/\varepsilon'_{RT} \le +22\%$ in a temperature range −55 to 125 °C) ceramic and a new method to identify Nd^{3+} ($3d^3$) and Ce^{3+} ($3d^1$) Kramers ions in ceramics via the room temperature (RT) ESR technique for their mixed site occupations.

* Corresponding author.
E-mail address: dylu@jlict.edu.cn (D.-Y. Lu).

https://doi.org/10.1016/j.matlet.2018.04.012
0167-577X/

2. Experimental procedure

The initial materials were reagent-grade $BaCO_3$, TiO_2, CeO_2 (Kanto Chem.) and Nd_2O_3 (Wako Pure Chem.). $(Ba_{1-x}Nd_x)(Ti_{1-y-x/4}Ce_y)O_3$ ($x = 0.03$, 0.04, 0.05, $y = 0.05$) (BNTC5) and ($x = 0.05$, $y = 0.06$) (BN5TC6) ceramics were prepared using the mixed oxide method, as described elsewhere [2]. Final sintering was 1450 °C for 24 h in air.

Powder X-ray diffraction (XRD) data were collected at RT using a Rint 2200 X-ray diffractometer (Rigaku). Crystal structures were determined by MS Modeling (Accelry) and Cu $K\alpha_1$ radiation ($\lambda = 1.540562$ Å). The microstructure was observed using a JSM-6330F scanning electron microscope (SEM) (JEOL) operated at 15 keV. Dielectric-temperature curves were measured using an AD-3521 FFT Analyzer (A&D); ac electric field: 10 V/mm; heating rate: 2 °C/min. ESR spectra were measured at RT using a JES-RE3X spectrometer (JEOL) at X-band frequency (9.148 GHz) in October 2006 and using an A300-10/12 spectrometer (Bruker) at 9.813 GHz in November 2017.

3. Results and discussion

Powder XRD patterns of BNTC5 and BN5TC6 ceramics are shown in Fig. 1. For simplicity, BNTC5 with $x = 0.03$, 0.04, and 0.05 are called BN3TC5, BN4TC5, and BN5TC5, respectively. These ceramic exhibited a pseudo-cubic perovskite structure. On the basis of a comparison in 12-coordinate ionic size between Ba^{2+} (1.61 Å) and Nd^{3+} (1.27 Å)/Ce^{3+} (1.34 Å) and in 6-coordinate ionic size between Ti^{4+} (0.605 Å) and Ce^{4+} (0.87 Å) [16], a decrease in

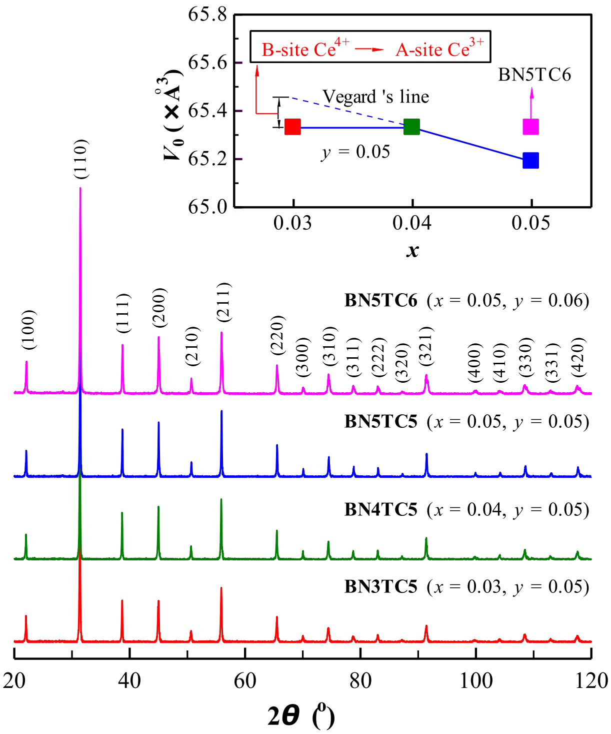

Fig. 1. Powder XRD patterns of BNTC5 and BN5TC6.

unit-cell volume (V_0) from $x = 0.04$ to 0.05 (Fig. 1 inset) provides evidence for the main occupations of B-site by Ce^{4+} and of A-site by Nd^{3+}. It is not easy for 6-coordinate Nd^{3+} (0.983 Å) to enter B-site because of its lager ionic size as compared to Ce^{4+}. The abnormal decline in V_0 at $x = 0.03$ compared to the Vegard's line (Fig. 1 inset) is most likely caused by the occupations of A-sites by some Ce^{3+} ions. The V_0 of BN5TC6 was higher than that of BN5TC5, which further confirms that Ce ions were mainly substituted on B-sites as Ce^{4+}.

SEM micrographs of BNTC5 and BN5TC6 are shown in Fig. 2. The thermal etching caused fracture of larger grains in BNTC5. The white particles possibly arose from liquid phases formed in sintering stage. BN5TC6 is similar to BL3TC5 in microstructure [2] and its average grain size determined by Fullman's method [2] is 1.8 μm.

Temperature dependences of dielectric permittivity (ε') and dielectric loss (tan δ) for BNTC5 and BN5TC6 are shown in Fig. 3. BNTC5 exhibited a diffuse phase transition (DPT [17]) behavior. The dielectric-peak temperature (T_m) decreased rapidly at a rate of −27 °C/at.% Nd (Fig. 3 inset), which is lower than that of $(Ba_{1-x}La_x)(Ti_{1-y-x/4}Ce_y)O_3$ ($y = 0.05$) (−30 °C/at.% La) [2]. BN5TC5 satisfied X7V specification but tan δ was very high (tan $\delta = 0.219$) because of its semiconducting nature. A high-permittivity ($\varepsilon'_{RT} = 14100$) and low-loss (tan $\delta = 0.014$) X7V ceramic was achieved in BN5TC6, indicating that the addition of 1% Ce in BN5TC5 can greatly reduce tan δ. Moreover, a comparison in ε'-T curves measured in 2006 and 2017 reveals that BN5TC6 possessed good ageing-resisting performance. The persistence of the shoulder at 299 cm^{-1} [B_1 + E(TO + LO)] in Raman spectrum (Fig. 4b inset) indicates local off-centering of B-cations and is consistent with the order-disorder nature of the ferroelecric-paraelecric phase transition in $BaTiO_3$. Some ferroelectric phases might exist in BN5TC6 and the macro-grains (Fig. 2) should play a crucial role in high-permittivity DPT behavior. The band at 834 cm^{-1} was caused mainly by A-site Nd^{3+}.

ESR spectra of BNTC5 and BN5TC6 are shown in Fig. 4. A $g = 2.004$ signal associated ionized Ti vacancies [18,19] was detected in 2006. The role of Ti vacancies is to apt to incorporation of larger Ce^{4+} ions into B-sites in sintering stage, a decrease in

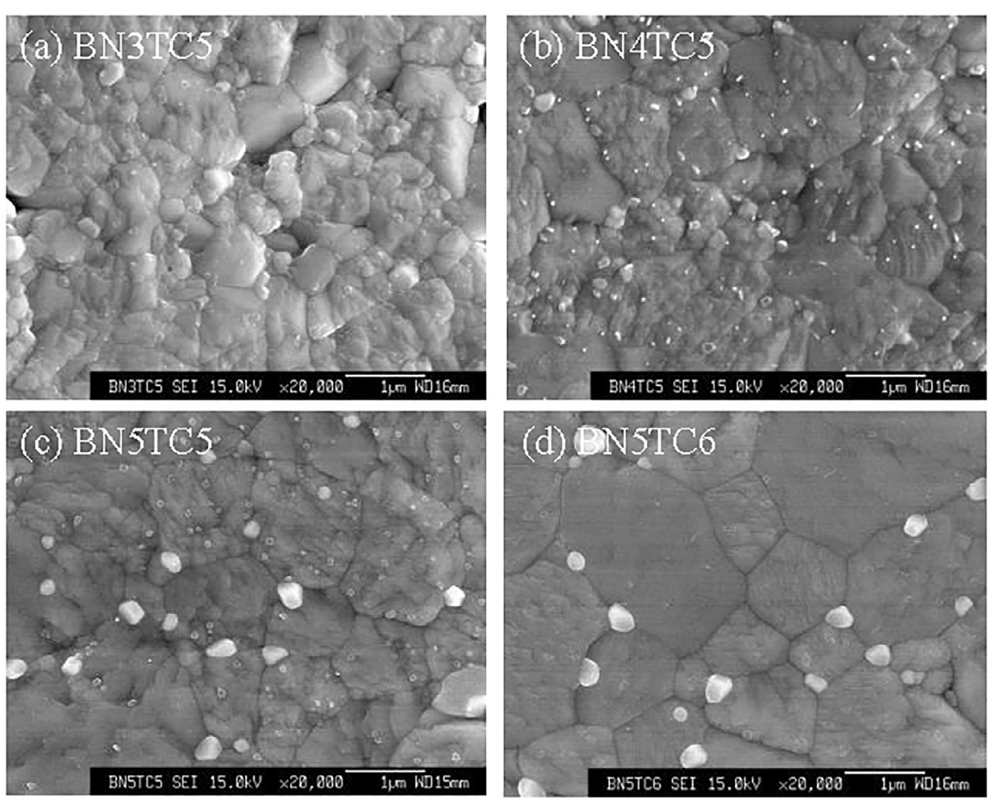

Fig. 2. SEM micrographs of the polished and thermally etched surfaces of BNTC5 with x = (a) 0.03, (b) 0.04, (c) 0.05; and (d) BN5TC6.